Discovery of quorum-sensing reprogramming determinants in *Pseudomonas aeruginosa* by a novel experimental evolution approach

Wenjie Cai[1,2], Huimin Liao[1,2], Mingqi Lu[1,2], Xiangting Zhou[1,2], Xiaoyan Cheng[1,2], Christian Staehelin[3], Weijun Dai[1,2]

[1]Guangdong Laboratory for Lingnan Modern Agriculture, South China Agricultural University, Guangzhou, 510642, China

[2]College of Plant Protection, Integrative Microbiology Research Center, South China Agricultural University, Guangzhou, 510642, China

[3]State Key Laboratory of Biocontrol and Guangdong Key Laboratory of Plant Resources, School of Life Sciences, Sun Yat-sen University, Guangzhou 510275, China

Send correspondence to: Weijun Dai

Integrative Microbiology Research Center, South China of Agricultural University, Guangzhou, 510642, China

daiweijun@scau.edu.cn

Running title: Identification of QS-reprogramming determinants

Key words: quorum sensing, LasR, *Pseudomonas aeruginosa*

Abstract

LasR is a master regulator of quorum-sensing (QS) in *Pseudomonas aeruginosa*. LasR-null mutants commonly appear in lung isolates from chronically infected cystic fibrosis (CF) patients. However, numerous such CF isolates have a QS-active phenotype, but factors underlying QS-reprogramming in LasR-null mutants remain largely unknown. Mutations in the transcriptional regulator gene *mexT* are well known to be responsible for QS-reprogramming in a laboratory LasR-null mutant strain, however, simultaneous occurrence of *lasR* and *mexT* mutations is rare in CF isolates. To identify QS-reprogramming determinants, we developed an experimental evolution approach, for which a QS-inactive LasR null mutant with an extra copy of *mexT* was engineered. In such a strain, spontaneous single *mextT* mutations are expected to have no or little phenotypic consequences. This novel method, named "targeted gene duplication followed by mutant screening" (TGD-MS), resulted in identification of QS-active revertants with mutations in genes other than *mexT*. We characterized a QS-active revertant with a point mutation in *rpoA*, a gene encoding the α-subunit of RNA polymerase. QS activation in this mutant was found to be associated with down-regulated expression of *mexEF-oprN* efflux pump genes. In an iterative TGD-MS experiment, we discovered mutations in *mexE*, a gene encoding a membrane fusion protein of the MexEF-OprN efflux pump. Our results implicate that a regulatory circuit controlling the expression of the *mexEF-oprN* operon is critical for QS-reprogramming. In conclusion, our study reports on identification of non-MexT proteins associated with QS-reprogramming in a laboratory strain, shedding light on possible QS activation mechanisms in clinical *P. aeruginosa* isolates. More generally, we describe a novel experimental evolution approach, in which the populations contain extra copies of previously identified genes. The TGD-MS method facilitates the identification of mutations in unknown genes and opens the perspective of iterative application. We suggest that this method can be employed to uncover untapped pathways in any transformable haploid organism.

Introduction

Pseudomonas aeruginosa is an opportunistic pathogen that causes severe acute and chronic human infections in cystic fibrosis (CF) patients with compromised immune system [1, 2]. A cohort of *P. aeruginosa* virulence factors is under the control of the quorum-sensing (QS) system [3, 4]. QS is a bacterial cell-cell communication system that regulates the expression levels of hundreds of genes in a cell density-dependent manner [4]. *P. aeruginosa* has two acyl-homoserine lactone (AHL) QS systems, the Las and Rhl QS systems. In the Las QS system, LasI catalyzes the diffusible QS signal *N*-3-oxododecanoyl homoserine lactone (3OC12-HSL), while the transcriptional regulator LasR binds to the 3OC12-HSL forming a protein-signal complex. The active 3OC12-HSL-LasR complex further activates Las-regulon genes. Similarly, Rhl QS contains an RhlI-RhlR pair, with RhlI synthesizing the butyryl-homoserine lactone (C4-HSL) and the C4-HSL-bound RhlR activating expression of the Rhl-regulon [5]. These two AHL QS systems further interact with the so-called *Pseudomonas* quinolone signal (PQS) system, which is responsible for generating 2-heptyl-3-hydroxy-4-quinolone (PQS) and its precursor 2-heptyl-4-quinolone (HHQ). The *pqs* genes (operon *pqsABCDE* and *pqsH*) code for HHQ and PQS synthesis [6, 7]. In general, the Las QS is at the top of the QS hierarchy, and disruption of either LasI or LasR diminishes the expression of QS-activated genes [4].

QS-active *P. aeruginosa* show QS-regulated responses such as production of extracellular proteases, C4-HSL, hydrogen cyanide, rhamnolipids and pyocyanin [8-11]. Secretion of QS-regulated proteases

allow the bacteria to be visualized on agar plated containing skim milk [12, 13]. Thus, spontaneous QS-active revertants derived from QS-inactive mutants can be selected on these agar plates. In such evolution experiments, mutants reprogramming their QS have been obtained from a QS-inacive *lasR* mutant of the laboratory strain PAO1 [14, 15]. Isolates with mutated *lasR* gene have been identified in CF patients with chronic *P. aeruginosa* infection [8, 16, 17]. However, although LasR is a master regulator of QS in *P. aeruginosa*, many LasR-null clinical isolates are QS-active (Bjarnsholt et al., 2010; Chen et al., 2019; Cruz et al., 2020; Feltner et al., 2016). Hence, QS-reprogramming of LasR-null mutants also appears to occur under natural conditions.

The *P. aeruginosa* genome encodes several resistance-nodulation-division (RND) multidrug efflux pumps that transport small molecules into the extracellular environment. One of them, the MexEF-OprN efflux pump, is suggested to regulate the QS system by exporting the PQS precursor HHQ which eventually leads to reduced intracellular PQS levels [18]. Furthermore, MexEF-OprN can export antibiotics such as chloramphenicol, fluoroquinolones and trimethoprim and thus contribute to antibiotic resistance [19]. The *mexT* gene is localized upstream of the *mexEF-oprN* operon. The MexT protein, a LysR-type transcriptional regulator, positively regulates *mexEF-oprN* expression [20]. In addition to the *mexEF-oprN* operon, MexT regulates expression of more than other 40 genes [21, 22]. Expression of *mexT* is negatively regulated by the neighboring gene *mexS* [23, 24]. Overexpression of the *mexEF-oprN* operon was found in various spontaneous *P. aeruginosa* mutants and results in reduced QS-related responses such as decreased synthesis of C4-HSL, hydrogen cyanide and pyocyanin [18, 25]. Mutations in the *mexT* gene were identified in clinical isolates from CF lungs and other patients with *P. aeruginosa* infections chronic CF lungs and other infection [16, 26] as well as in *P. aeruginosa* laboratory strains [27, 28]. In a QS-inactive LasR-null mutant of the laboratory strain PAO1, MexT inactivating spontaneous mutations in *mexT* were found to be sufficient for QS-reprogramming [14, 15], indicating that reduced expression of the *mexEF-oprN* genes is associated with a functional QS [21, 29]. Likewise, disruption of the MexEF-OprN efflux pump in the LasR-null mutant background results in a QS-active phenotype with a functional Rhl QS as well as an active PQS system [14, 15]. Accordingly, deletion of genes of the PQS system (*pqsA* and/or *pqsE*) causes partially attenuated QS-dependent responses [14]. Although mutations in *mexT* were frequently obtained in laboratory experiments, they are rare in clinical isolates [16]. For example, a LasR-null isolate from a CF patient with chronic infection showed a QS-active phenotype while containing a functional MexT [9]. Therefore, QS-reprogramming in such clinical isolates is expected to be controlled by factors other than MexT inactivation (none-*mexT* mutations).

In this study, we developed a novel experimental evolution approach to identify none-*mexT* determinants involved in QS-reprogramming. A QS-inactive *P. aeruginosa* LasR null mutant with an extra copy of *mexT* was generated and then used to screen for QS-active revertants. In this way, we identified a QS-active mutant with a spontaneous mutation in the transcriptional regulator gene *rpoA*. Further experiments showed that RpoA is involved in a regulatory circuit controlling the expression of the *mexEF-oprN* operon and thus critical for QS-reprogramming. In an iterative evolution experiment with a LasR null mutant containing extra copies of *mexT* and *rpoA*, we identified a QS-active revertant with mutated *mexE*, a gene encoding a membrane fusion protein of the MexEF-OprN efflux pump. Hence, the developed mutant screening method resulted in identification of novel *P. aeruginosa* genes associated with MexEF-OprN efflux pump function and QS-reprogramming.

Results

Simultaneous occurrence of *lasR* and *mexT* mutations is rare in *P. aeruginosa* CF isolates

LasR mutants are common in *P. aeruginosa* isolates from CF patients with chronic infection. These CF isolates contain an active Rhl QS [8, 11]. In evolution experiments with QS-inacive LasR mutants of the laboratory strain PAO1, QS-active revertants were screened on skim milk agar plates and identified to have with *mexT* mutations [14, 15]. However, it is unclear whether such QS-reprogramming also applies to clinical isolates. To address this concern, we re-analyzed previously published whole genome sequencing (WGS) data of *P. aeruginosa* CF isolates with respect to *lasR* and *mexT* mutations (Smith et al., 2006). Among CF isolates from 29 patients examined, *lasR* mutations, including frameshift mutations, single nucleotide substitutions and insertions, were identified in isolates from 22 patients (75.9%). However, only isolates from two patients (9.1%) simultaneously had nonsynonymous mutations in *lasR* and *mexT* (Fisher's exact test, P = 0.23, odds ratio = 0.27). Moreover, *mexT* mutations were additionally found in a number of isolates that contain an intact *lasR* (Table S1). Hence, *mexT* mutations are frequently not colocalized with *lasR* mutations in the examined WGS data. Therefore, inactivation of MexT might often not account for QS activity in clinical LasR-null isolates possessing a QS-active phenotype. In accordance with these findings, Cruz et al. (2020) reported on a QS-active clinical isolate which was identified as LasR-null isolate with a functional *mexT* gene.

Transposon mutagenesis results in a QS-active LasR null mutant with mutated *mexF* gene

To explore uncharacterized QS factors responsible for QS-reprogramming, we first performed a traditional transposon mutagenesis experiment using a *mariner*-based transposon (pBT20) [30] and a QS-inactive LasR null mutant of strain *P. aeruginosa* PAO1. The constructed insertion mutant library was spread on skim milk agar. In this screening approach, QS-active mutants were selected basing on the secretion of QS-related proteases. A total of 40, 000 mutant colonies, corresponding to a transposon density of about 156 bp per insertion in the PAO1 genome, were examined. Using this screening method, we obtained a single bacterial colony with a protease-positive phenotype. Sequencing analysis indicated that this mutant possesses a transposon insertion in the *mexF* gene, which codes for an essential component of the MexEF-OprN efflux pump. Given that QS-reprogramming in LasR null mutants mostly relies on mutations in *mexT* [14, 15], it was not surprising to see that a disruption of MexF results in a QS-active phenotype. However, no other genes involved in QS-reprogramming were identified using this transposon mutagenesis method.

A novel experimental evolution method for identification of QS-reprogramming genes

Considering *P. aeruginosa* has an intriguing capacity for adapting to environments through frequent genome variations (Huang et al., 2019), we expected that hitherto unknown genetic elements involved in QS-reprogramming can be identified in evolution experiments. In a classic approach, a QS-inactive LasR-null mutant is evolved in casein medium and spontaneous mutants emerge. The QS-active phenotype of the protease-positive revertants can then be confirmed by measuring production of various QS-related metabolites such as pyocyanin. Using this approach, sequencing of QS-active mutants resulted only in mutations in the *mexT* gene [14, 15]. We therefore developed a new approach in which the probability of obtaining *mexT* mutations was reduced by introducing an extra copy of *mexT* into a neutral site of the LasR mutant genome. We assumed that a deleterious mutation in one copy of

the two *mexT* genes would still leave the other copy functional and therefore would have no or little phenotypic consequences in the evolution experiment. Using this strategy, mutants with single *mexT* mutations are expected to be largely filtered out, thereby facilitating the identification of non-*mexT* mutations. The method, termed targeted gene duplication followed by mutant screening" (TGD-MS), is schematically illustrated in Fig. 1.

The TGD-MS method results in identification of a QS-active LasR null mutant with a mutation in *rpoA*

Using the established TGD-MS strategy, we screened for QS-active mutants of the engineered LasR-null mutant carrying two *mexT* copies. Mutants were further characterized with respect to confirmation of protease activity using a skim milk agar assay and pyocyanin production. Four protease-positive mutants were found to show significantly increased pyocyanin production, providing clues for an active QS (Fig. 2). Three of these mutants were then subjected to whole-genome re-sequencing (WGS). The sequencing results revealed that these colonies possess a common single nucleotide mutation (nucleotide T4754641→C; amino acid residue T262→A) in *rpoA* (Table S2 and S3). The *rpoA* gene encodes the α-subunit of RNA polymerase (RNAP) in *P. aeruginosa*. Since *rpoA* is essential for cell viability in *P. aeruginosa* [31], a deletion mutant of *rpoA* has not been reported in the literature.

To elucidate the role of *rpoA* in QS regulation, the same point mutation (T262→A) was introduced into the LasR-null mutant, generating the mutant LasR-RpoA-T262A (hereafter designated as LasR-RpoA* and the RpoA-T262A protein as RpoA*). As expected, LasR-RpoA* displayed a typical QS-active phenotype with respect to extracellular protease activity as visualized on skim milk agar plates (Fig. S1). Furthermore, compared to the QS-inactive LasR-null mutant, LasR-RpoA* showed increased Rhl- and PQS-responsive activities as determined by reporter plasmids as well as elevated production of C4-HSL, PQS, pyocyanin and hydrogen (Fig. 3). Overall, the QS-dependent activities and metabolites of the LasR-RpoA* mutant were higher than those of the LasR-null mutant, but lower compared to a constructed QS-active LasR-MexT double mutant (*mexT* deletion mutant of LasR) (Fig. S1 and Fig. 3). Cell killing activity was also higher for LasR-RpoA* in comparison with the LasR-null mutant (Fig. S2). Complementation of the LasR-RpoA* mutant with an episomal copy of wild-type *rpoA* reduced the extracellular protease activity and pyocyanin production to levels determined for the LasR-null mutant carrying the empty vector (Fig. S3). In conclusion, application of the TGD-MS method resulted in identification of RpoA as a novel regulator of QS-controlled processes.

The LasR-RpoA* mutant exhibits a QS-active transcriptome profile

To investigate gene expression changes in the LasR-RpoA* mutant related to QS activation, we performed an RNA-sequencing (RNA-seq) analysis and compared the trancriptome profiles of LasR-RpoA* with that of the parent strain LasR-null. Overall, global gene expression was induced in the LasR-RpoA* mutant compared to LasR-null, with a total of 182 genes differentially expressed (at least a 2-fold change, $P < 0.05$) (Fig. 4A and Table S4). Regarding the expression of QS-related genes, *rhlI* (encoding acyl-homoserine-lactone synthase) was weakly upregulated and the *pqs* operon genes required for PQS production showed strong induction (Fig. 4B and Table S4). This transcriptome profile confirmed that the LasR-RpoA* mutant has an active Rhl and PQS QS system. Reduced

expression of genes of the *mexEF-oprN* caused by *mexT* mutations has been reported to lead to QS-reprogramming in the LasR-null background [14, 15]. Likewise, in comparison with the LasR-null mutant, the LasR-RpoA* mutant showed substantially decreased expression of genes encoding the MexEF-OprN efflux pump (Fig. 4C and Table S4). Quantitative real-time PCR (qRT-PCR) analysis of selected QS-related genes and *mexEF-oprN* operon genes confirmed the data obtained by RNA-seq (Fig. S4).

Next, we compared the transcriptome profiles of the LasR-MexT and LasR-null mutants. A total of 297 genes were found to be differentially expressed (Table S5). In accordance with a previous study [22], many differentially expressed genes in the LasR-MexT mutant were related to the MexEF-OprN efflux pump. Genes with at least 4-fold up-regulation in the LasR-MexT mutant were then selected for a further comparison with the identified differentially expressed genes in the LasR-RpoA* mutant. These genes showed also induced expression in the LasR-RpoA* mutant (P = 0.01, one-sided Kolmogorov-Smirnov (KS) test). In contrast, no clear difference was observed for down-regulated genes (P = 0.07, one-sided KS test). Because the MexEF-OprN efflux pump negatively regulates QS activity [32], our transcriptome analysis supports the view that QS-reprogramming in LasR-RpoA* and LasR-MexT is associated with reduced *mexEF-oprN* operon gene expression in both mutants.

The RpoA* protein modulates transcription of *mexEF-oprN* operon genes

We used a green fluorescent protein (GFP) based transcriptional fusion system (P*mexE*-GFP) to estimate the promoter activity of *mexEF* in PAO1 derivatives (core promoter of the *mexEF-oprN* operon). In line with the results obtained from RNA-seq and qRT-PCR analysis, the presence of the RpoA* protein in LasR-RpoA* carrying the reporter construct caused a sharp reduction of fluorescent signals, indicating reduced expression of the *mexEF-oprN* operon genes (Fig. 5A). However, an even stronger reduction of fluorescent signals was observed for LasR-MexT mutant carrying the reporter construct (Fig. 5A). These findings are in agreement with the observation that QS-related activities are weaker in LasR-RpoA* than in LasR-MexT (Fig. 3). Furthermore, we analyzed the LasR-RpoA* mutant with respect to swarming motility as inactivation of the MexEF-OprN efflux pump was reported to stimulate swarming motility (Lamarche and Déziel, 2011). As expected, the LasR-RpoA* was found to exhibit considerably increased swarming motility when compared to the LasR-null parent strain (Fig. S5).

We next examined how RpoA* attenuates expression of the *mexEF-oprN* operon genes. As the RpoA protein is a transcriptional regulator, we hypothesized that the RpoA* protein may directly interfere with the binding of RNAP to the *mexEF* promoter. To test this hypothesis, we performed an electrophoretic mobility shift assay (EMSA). His-tagged RpoA or RpoA* was expressed in the LasR-RpoA* mutant. The recombinant RNAP proteins containing the His-tagged α-subunit were then extracted and purified by affinity chromatography. The two different types of RNAP were then tested for their ability to bind to a 243-bp *mexEF* promoter DNA probe (Fig. 5B). Both RNAP proteins bound to the probe in the EMSA (Fig. 5C). Compared to RNAP containing RpoA, however, a weaker signal was observed for RNAP containing the RpoA* variant, which indicates a reduced RNAP-probe interaction. We therefore concluded that RNAP containing RpoA* down-regulates expression of *mexEF-oprN* operon genes by reducing the direct contact of RNAP to the *mexEF* promoter DNA.

The LasR-RpoA* mutant is fitter than the LasR-MexT mutant in the presence of chloramphenicol

Chloramphenicol is a known antibiotic substrate of the MexEF-OprN efflux pump [33]. We therefore investigated whether the identified mutation in *rpoA* affects antibiotic resistance, shedding light on the relationship between QS and antibiotic resistance in clinical *P. aeruginosa* isolates. Since a functional MexEF-OprN efflux pump promotes antibiotics resistance [25, 34], we suggested that the arising LasR-RpoA* mutant from the neighboring LasR-null mutant would be fitter than the LasR-MexT mutant when the bacteria are exposed to chloramphenicol. To test this hypothesis, we examined the ability of LasR-RpoA* to compete with LasR-null using casein-based broth containing different concentrations of chloramphenicol. As expected, growth of LasR-RpoA* relative to LasR-null was reduced with increasing concentrations of chloramphenicol, indicating that chloramphenicol represses the growth advantage of LasR-RpoA*. Similar competition tests were also performed with the LasR-MexT and LasR-null mutants. Increasing chloramphenicol concentrations caused strongly reduced growth fitness of LasR-MexT relative to LasR-null. Notably, growth fitness reduction of LasR-MexT was even more pronounced than that of LasR-RpoA* (Fig. 6). In conclusion, our findings indicate that the LasR-RpoA* is relatively fitter than the LasR-MexT mutant when emerging through QS-reprogramming from the LasR-null parent strain in the presence of chloramphenicol.

PQS production contributes to RpoA*-mediated QS activation

Previous findings showed that inactivation of the MexEF-OprN efflux pump up- QS-dependent activities by reducing the export of the PQS precursor HHQ [18, 32], which may contribute to increased PQS production in LasR-RpoA* and LasR-MexT mutants (Fig. 3D). As *pqsA* codes for a coenzyme ligase essential for PQS biosynthesis [35], we deleted the *pqsA* gene in the LasR-RpoA* mutant (LasR-RpoA*-PqsA) and evaluated the mutant's ability to secrete proteases. The *pqsA* deletion caused a strong but not complete reduction of the QS-controlled extracellular protease activity (Fig. S6). In conclusion, the obtained results suggest that QS-reprogramming in the LasR-RpoA* mutant partially depends on increased PQS production.

Iterative use of the TGD-MS method

Our TGD-MS experiment showed that introduction of an extra copy of *mexT* into LasR-null helped to identify a QS-active revertant with a mutation in *rpoA*. To find more QS-reprogramming genetic determinants, we performed an iterative evolution experiment. We again used the TGD-MS method and constructed a LasR-null derivative with extra copies of *mexT* and *rpoA*. We hypothesized that an evolution experiment with such a strain might result in a QS-active mutant with a mutation in a gene other than *mexT* or *rpoA*. Using this approach, we identified a QS-active mutant with mutated *mexE* coding for a membrane fusion protein of the MexEF-OprN efflux pump [25]. Previous work showed that disruption of MexE in a QS-inactive LasR-null mutant is sufficient to obtain a QS-active phenotype [14]. Therefore, QS-reprogramming in a LasR-null mutant may depend either on defects in positive regulators of the *mexEF-oprN* operon (MexT, RpoA) or on malfunction of the MexEF-OprN efflux pump (MexE and MexF). Fig. 7 illustrates the regulatory process controlling transcription of *mexEF-oprN* operon genes. Taken together, our results suggest that the TGD-MS method can be used iteratively in evolution experiments to detect mutations in previously unknown genes. We suggest that this method can be generally employed to uncover untapped pathways in any transformable haploid organism (Fig. 8).

Discussion

A novel approach, named TGD-MS, was used in the evolution experiments of this study to discover mutations in genes involved in QS-reprogramming in a LasR-null mutant of *P. aeruginosa*. In the present study, TGD-MS approach was used for obtaining QS-active revertants. By constructing a strain containing an extra copy of *mexT*, QS-active revertants carrying a mutated *mexT* gene could be filtered out to a large extent in our screen for QS-reprogramming mutants. Using this increased screening stringency, a QS-active mutant with a single nucleotide substitution in *rpoA* was identified. Likewise, a *mexE* was obtained in an iterative evolution experiment using a LasR-null population with extra copies of *mexT* and *rpoA*. It is worth noting in this context that it would have been impossible to identify the QS-reprogramming function of RpoA by conventional transposon insertional mutagenesis, because *rpoA* is an essential gene for cell viability [31]. More generally, The TGD-MS method described in this work allows to elucidate the genetic components of known pathways and even to reveal unknown metabolic pathways. The use of the TGD-MS method in evolution experiments is now opening up new opportunities for scientists to make fundamental discoveries in a wide range of research areas. We hypothesize that the TGD-MS method can be employed to uncover genetic components of known and unexplored pathways in any transformable haploid organism.

Our study on a QS-inactive LasR-null mutant of *P. aeruginosa* uncovers a novel QS-reprogramming role for RpoA, which is an essential subunit of the bacterial RNAP. Adaptive mutations in *rpoA* have been found to be beneficial for bacterial growth in evolution experiments with different organisms [36, 37]. Previous publications showed that mutations in *rpoA* of *Bacillus subtilis* and *Escherichia coli* promote the utilization of secondary carbon sources and ribosome synthesis [38]. The QS-related function of RpoA* found in the present study implicates that that the T262 to A substitution of this protein variant leads to a structural modification in RpoA which affects the interaction between RNAP and the promoter DNA of the *mexEF-oprN* operon (Fig. 5). These findings are in agreement with previous studies on bacteria that certain residues in the α-CTD domain of RpoA are important for promoter contact, while a subset of these residues is required for the interaction with transcriptional effectors [39-41]. Overall, our results of our study suggest that a minor structural change in RpoA caused by a single point mutation restores QS-dependent activities in a LasR-null mutant, thereby allowing adaptation to rapidly changing environments.

LasR-MexT mutants of *P. aeruginosa* exhibit low expression of the *mexEF-oprN* operon, suggesting that weak or absent protein levels of the MexEF-OprN efflux pump lead to QS-reprogramming in evolution experiments [14, 15]. Similarly, the QS-active LasR-RpoA* mutant in our study showed QS-related activities and transcriptome changes, including reduced expression of *mexEF-oprN* operon genes. Our transcriptome analysis, EMSA and the QS-active phenotype of the LasR-RpoA* mutant collectively suggest that RpoA* affects the QS network through expression of *mexEF-oprN* operon genes. The MexEF-OprN efflux pump can export the PQS precursor HHQ and inactivation of this pump is therefore may increase PQS levels in the cell, resulting in induction of PQS-related QS responses [18, 32]. However, deletion of key components of the PQS system, such as PqsA and/or PqsE [6, 35], only partially reduced QS activity in a LasR-MexT mutant [14]. Similarly, the LasR-RpoA*-PqsA mutant deficient in PQS synthesis was found to possess weak but detectable QS activity in the present study, indicating that the RpoA*-mediated QS activation in LasR-RpoA* is partially independent of

the PQS system (Fig. S5).

Multidrug-resistance pumps of the RND family play key roles in bacterial resistance against antibiotics [42]. The *mexEF-oprN* operon of *P. aeruginosa* codes for a typical RND efflux pump, which renders the bacterium largely resistant to chloramphenicol, fluoroquinolones and trimethoprim [19]. On the other hand, the MexEF-OprN efflux pump can also export HHQ and overexpression of *mexEF-oprN* operon genes resulted in reduced QS-related activities [18, 32]. Thus, protein levels of this efflux pump may ultimately affect QS-controlled bacterial virulence of clinical *P. aeruginosa* isolates. Previous studies reported that CF patients possess QS-active LasR-null strains in their lungs [8, 10, 11]. *P. aeruginosa* isolates from chronically infected CV patients often develop antibiotic resistance because they receive continuous high doses of antibiotics over a long period of time [43]. In other words, expression of efflux pump genes is required for antibiotic resistance but impairs QS circuits that control the production of bacterial virulence factors. This raises the question of how QS-inactive LasR-null mutants resolve the dilemma between antibiotic resistance and QS-reprogramming. The findings of this study highlight that the MexEF-OprN efflux pump is at the center of this tradeoff between antibiotic resistance and QS-controlled virulence factor production. The single amino acid substitution in RpoA* caused reduced expression of *mexEF-oprN* operon genes in our study. Accordingly, when compared with the LasR-MexT mutant, the LasR-RpoA* mutant was found to have relatively higher growth fitness in competing the LasR-null parental strain when the bacteria were exposed to increasing concentrations of chloramphenicol (Fig. 6). In conclusion, our work shows that a mutation in *rpoA* can fine-tune the efficiency of an RND efflux pump required for antibiotic resistance and efflux of HHQ, thereby modulating antibiotic resistance and production of QS-dependent virulence factors under varying environmental conditions. How the MexEF-OprN efflux pump affects the relationship between antibiotic resistance and QS-dependent bacterial virulence should be further investigated in the future.

P. aeruginosa possesses a complicated regulatory gene network to control expression of virulence genes [44] and undergoes evolutionary changes in the phase of chronic CF infection [43]. In our TGD-MS approach for example, when an extra copy of *mexT* was inserted into a LasR-null mutant, we observed that the bacterium can activate MexT-independent alternative QS-reprogramming pathways. Given that MexT controls not only expression of *mexEF-oprN* operon genes but also transcription of potentially important virulence genes [21, 22], it can be speculated that maintaining a non-modified MexT is critical for survival in chronically infected CF patients. Notably, our *mexT* sequence analysis and previous observations indicate that numerous LasR-null, QS-active *P. aeruginosa* isolates from CF patients retain a functional MexT [9, 16]. Taken together, we report in this study on a novel experimental evolution approach which facilitated identification of non-*mexT* genes involved in formation of the MexEF-OprN efflux pump and QS-reprogramming. Future research is needed to identify similar mutations in clinical isolates and to clarify their effects on QS activities, virulence and antibiotic resistance.

Materials and methods

Bacterial strains and growth conditions

Pseudomonas aeruginosa wild-type strain PAO1 and the LasR-null mutant (Wang et al., 2015) used in this study were obtained from E. Peter Greenberg (University of Washington, USA). *P. aeruginosa* PAO1 and mutant derivatives (Supplementary Table S6) were grown in Luria Bertani (LB) broth

(containing 10 mg/ml tryptone, 5 mg/ml yeast extract, 10 mg/ml NaCl) at 37°C. LB broth was buffered with 50 mM 3-(N-morpholino) propanesulfonic acid, pH 7.0 (LB-Mops broth). The photosynthetic medium (PM) [45] supplemented with 1% sodium caseinate (Sigma Aldrich, St. Louis, MO, USA) as the sole carbon source (PM-casein medium) was used for evolution experiments at 37°C. Unless otherwise specified, *P. aeruginosa* strains were cultured in 14-mL Falcon tubes (Corning Inc., Corning, NY, USA) containing 3 ml medium, with shaking (220 rpm) at 37°C. *Escherichia coli* was grown in LB broth at 37°C. Details on bacterial strains and plasmids used in this study are shown in Supplementary Table S6.

Construction of *P. aeruginosa* mutants

Construction of *P. aeruginosa* mutants (LasR-MexT with *mexT* deletion, LsR-RpoA* mutant with a *rpoA* point mutation (T262→A), LasR-RpoA*-PqsA with a *pqsA* deletion) was performed according to a homologous recombination approach described previously [46]. Briefly, about 500 ~ 1000 bp of DNA flanking the targeted single nucleotide substitution or the full length gene of interest were PCR-amplified and cloned into the pEXG-2 vector containing a gentamycin (Gm) resistance gene [46, 47] using the Vazyme ClonExpress II One Step Cloning Kit (Vazyme Biotech, Nanjing, China). The constructed plasmids were then mobilized into *P. aeruginosa* (LasR-null and LasR-RpoA*, respectively) by triparental mating with the help of *E. coli* carrying the helper plasmid pRK2013 (Figurski and Helinski, 1979). Mutants were first selected on *Pseudomonas* Isolation Agar (PIA) containing Peptic digest of animal tissue 20.0 g/L,Magnesium chloride 1.4 g/L, Potassium sulfate 10.0 g/L, Triclosan (Irgasan) 0.025 g/L, and Agar 13.6 g/L supplemented with 100 μg/ml Gm and then on LB agar containing 10% (w/v) sucrose. All mutants were confirmed by PCR amplification and subsequent DNA Sanger sequencing. The primers used in this study are listed in Supplementary Table S7.

Complementation of the LasR-RpoA* mutant

The *rpoA* gene was cloned into the pJN105 expression vector with the Vazyme ClonExpress II One Step Cloning Kit, generating plasmid pJN105-*rpoA*. The constructed plasmid and the empty vector pJN105 as a control were then mobilized into the LasR-RpoA* mutant by triparental mating. The bacteria were grown in LB-Mops broth at 37°C. Expression of *rpoA* in the complementation strain was induced by addition of 1 mM L-arabinose and the bacteria were harvested 20 h later.

Evolution experiments

Three independent colonies of the LasR-null mutant carrying a miniTn7-MexT construct at a neutral site of the genome were separately inoculated into 3 ml LB-Mops broth to obtain an overnight culture. 100 μL of the bacterial suspension were then transferred into 3 ml PM-casein medium in 14-mL Falcon tubes (Corning). One passage was performed every 5 days by transferring 100 μL of bacterial suspension into 3 ml fresh PM-casein medium. When required, water was added to compensate for evaporated medium. The bacterial suspensions were then spread on LB agar plates. Finally, to visualize extracellular protease activity of the obtained colonies, the bacteria were subjected to a skim milk assay. An initial evolution experiment with a non-modified LasR-null mutant population (carrying a single *mexT* gene copy) was performed in a similar way. Furthermore, an iterative evolution experiment was performed with a LasR-null mutant carrying miniTn7-*mexT* and an additional miniTn7-*rpoA* construct.

Skim milk assay

Total extracellular proteolytic activity of *P. aeruginosa* strains was evaluated using skim milk agar plates on which the bacteria form a protease-catalyzed clearing zone surrounding each colony. Individual colonies were grown on LB agar and then spotted on the skim milk agar plates (25% (v/v) LB, 4% (w/v) skim milk, 1.5% (w/v) agar). Colonies with extracellular proteolytic activity formed clearing zones after incubation at 37°C for 24 h. The area of transparent zones reflecting extracellular proteolytic activity was quantified from captured photographs.

Pyocyanin measurement

Overnight cultures of *P. aeruginosa* grown in LB-Mops broth were diluted into 4 ml *Pseudomonas* P broth (20 g/L pancreatic digest of gelatin, 1.4 g/L magnesium chloride, 10 g/L potassium sulfate) to reach a starting OD_{600}≈0.02. The bacteria were cultured at 37°C for 20 h. The cells were then centrifuged at 16,000 g × 2 min. The culture supernatants were collected and their OD values at 695 nm were photometrically determined at 695 nm. Pyocyanin production was estimated by determining OD_{695}/OD_{600} values over time.

Hydrogen cyanide measurement

A test paper method was used to detect hydrogen cyanide produced by *P. aeruginosa* strains. A circle of a Whatman 3MM chromatography paper corresponding to the size of an agar plate was soaked in the HCN detection reagent consisting of 5 mg copper(II) ethyl acetoacetate 5 mg 4,4'-methylenebis-(N,N-dimethylaniline) mixed with chloroform (1 to 2 ml). *P. aeruginosa* cells grown overnight in LB-Mops broth were used to spot-inoculate 2% (w/v) peptone agar plates. After incubation at 37°C for 12 h, the plates were overlaid with the prepared test paper and incubated at 37°C for additional 12 h. The color of the paper turned blue when it was exposed to hydrogen cyanide. Image J software (https://imagej.nih.gov/ij) was used to quantify the production of hydrogen cyanide.

Swarming motility assay

P. aeruginosa strains were cultured in LB-Mops broth overnight to reach an OD_{600}≈1.8. Each bacterial suspension (1.5 μL; OD_{600} adjusted to 0.5) was then transferred to the center of an agar plate containing 0.5% (w/v) Bactor-agar, 8g/L nutrient broth (BD, CA, USA) and 5 g/L glucose. Bacteria were incubated at 37°C for 16-18 h.

Labeling of miniTn7-Gm

The pUC18T-mini-Tn7T-Gm (NCBI accession number: AY599232) [48]was integrated into a neutral site of the PAO1 genome by triparental mating using the helper plasmid pTNS2 (NCBI accession number: AY884833). The integration event was confirmed by PCR amplification and DNA sequencing. The excision of the Gm resistance gene was performed with the pFLP2 plasmid (NCBI accession number: AF048702) [48] and selection on LB agar containing 5% (w/v) sucrose.

Assays with strains containing reporter plasmids

Plasmids with a *rhlA* promoter-GFP fusion [8] and a constructed *pqsA* promoter-GFP fusion were used to

quantify the RhlR- and PQS-responsive activities, respectively. A plasmid containing a *mexE* promoter-GFP construct was used to assess the expression of the *mexEF-oprN* operon. The reporter plasmids were mobilized into *P. aeruginosa* strains and selected on LB agar plates (containing Gm). PAO1 strains carrying QS reporter plasmids were grown in LB-Mops broth containing 50 mg/ml Gm for 12 h. The bacterial suspensions were then diluted to LB-Mops broth containing 50 mg/ml Gm (OD_{600} ≈ 0.02) and grown for 18 h to stationary phase. Finally, the bacteria were transferred to 96-well plates (200 µl/well) with three technical replicates. Fluorescence (excitation 488 nm, emission 525 nm) and optical density (OD_{600}) values of the samples were determined using a microplate reader (Synergy H1MF, BioTek Instruments, Winooski VT, USA).

Quantification of C4-HSL and PQS

P. aeruginosa strains were cultured overnight in LB-Mops broth. Bacteria were then grown in 4 ml LB broth at 37°C for 18 h (starting OD_{600}≈0.02). AHLs were extracted with an equal amount of ethyl acetate. A bioassay with the reporter *E. coli* strain containing the pECP61.5 with a *rhlA-lacZ* fusion and an IPTG-inducible *rhlR* [8] was used to quantify C4-HSL in the ethyl acetate extract. Precise quantification of PQS was performed by LC/MS as described previously [35]. 10 µl of the ethyl acetate phase was subjected to liquid chromatography-mass spectrometry (LC-MS) analysis. The detection system (Q-Exactive Focus/Ultimate 3000; Thermo Fisher Scientific, Waltham, MA, USA) was equipped with a 100 x 2.1 mm, 1.7 µm ACQUITY UPLC HSS T3 chromatographic column (Waters, Milford, MA, USA). An acidified (1% glacial acetic acid by volume) water/methanol gradient was used as the mobile phase (0.4 ml/min flow rate; 40°C). PQS was quantified by measuring the area of PQS peaks in chromatograms from different samples and values were standardized according to the concentration of an added internal standard.

Production and purification of RpoA proteins

Full-length of His-tagged RpoA or the RpoA* variant was cloned into pJN105 expression vector. The plasmid was then mobilized into the LasR-RpoA* mutant and protein expression was induced by growth in LB broth containing 1 mM L-arabinose at 37°C for 18 h. Cells were pelleted at 13,000 g × 5 min and resuspended in lysis buffer (PBS buffer supplemented with 1×Protease Inhibitor Cocktail (Bimake, Houston, TX, USA), 1mg/ml lysozyme). Resuspended cells were lysed in a high pressure cell homogenizer machine (Stansted Fluid Power Ltd, Essex, United Kingdom) at 420 MPa. The lysed cells were centrifuged at 13,000 g × 5 min (4°C). The supernatant was then incubated with Ni-NTA beads (Qiagene, Shanghai, China) at 4°C for 2 h. The mixture was loaded on a chromatographic column, washed with washing buffer (500 mM NaCl, 20 mM NaH_2PO_4, 20 mM imidazole, pH 8.0), and finally eluted with a buffer containing high concentrations of imidazole (500 mM NaCl, 20 mM NaH_2PO_4, 250 mM imidazole, pH 8.0). Collected fractions were assessed by SDS PAGE analysis. Fractions containing recombinant protein were pooled and concentrated with an ultrafiltration device (MilliporeSigma, Burlington, MA, USA) and finally eluted with PBS buffer. Samples were stored at -80°C.

Electrophoretic mobility shift assay (EMSA)

The promoter sequence of the *mexEF-oprN* operon (P*mexE*) was used as probe for EMSA. The probe DNA was labeled with biotin Biotin-11-UTP (Jena Bioscience, Jena, Germany) through PCR amplification using T4 DNA polymerase (Novoprotein, Suzhou, China)). The labeled probe (30 ng) was incubated with 0.2 μg purified His-tagged RpoA or RpoA* protein in binding buffer (10 mM Tris-HCl, 50 mM KCl, 1 mM DTT, 1% (v/v) glycerin, 10 mM $MgCl_2$, 1 μg/μL poly(deoxyinosinic-deoxycytidylic) acid, pH 7.5) at room temperature for 30 min. The samples containing a given DNA-protein complex were subjected to electrophoresis on a 5% polyacrylamide gel in 0.5×Tris-borate-EDTA (TBE) buffer at 100 V for 180 min. DNA subsequently was transferred to a nylon membrane and incubated with milk blocking buffer (50 g/L milk powder in TBST buffer (50 mM Tris, 150 mM NaCl, 0.05% Tween-20, pH 7.5) for 30 min with shaking at room temperature. The membrane was then incubated with streptavidin-horseradish peroxidase conjugate (Thermo Fisher Scientific) in blocking buffer for 30 min at room temperature. The membrane was subsequently washed with TBST buffer for 4 times, 5 min each. DNA was visualized using the Immobilon Western kit (Millipore) and photographed by a Tanon 5200 Multi-Imaging System (Tanon, Shanghai, China).

Mammalian cell cytotoxicity assay

Human A549 cells were cultured in DMEM medium (GIBCO; Thermo Fisher Scientific) and F-12 medium (GIBCO) supplemented 10% FBS (GIBCO), respectively at 5% CO_2 and 37°C. Exponentially growing *P. aeruginosa* bacteria cultured in LB broth (OD_{600}≈1.0) were collected by centrifugation (6,000 g × 5 min) and washed with PBS. Next, the cells were added to near-confluent A549 cells at a starting multiplicity of infection (MOI) ratio of 10: 1. After incubation at 37°C for 8 h, the extent of cell killing was determined by quantification of the release of lactate dehydrogenase into the cell culture supernatant using the LDH Cytotoxicity Detection Kit (Beyotime, Nantong, China).

Competition experiment

The *P. aeruginosa* strains (LasR-null, LasR-RpoA* and LasR-MexT) were grown in PM medium supplemented with 0.5% (w/v) casein amino acids (Sangon, Shanghai, China) overnight and then transferred to liquid PM-Casein medium (adjusted to OD_{600}≈0.02) with or without chloramphenicol. Each strain tagged with a pUC18T-mini-Tn7T-Gm construct was cocultured with the non-tagged strain at a starting ratio of 5:95. The mixed cells were then grown at 37°C for 48 h. Cell counts were determined by spreading the bacteria onto LB agar plates supplemented with or without 10 μg/ml Gm. The relative fitness of each strain was deduced from the ratio of Malthusian growth parameters (w) = $\ln(X_1/X_0)/\ln(Y_1/Y_0)$, as defined previously [49].

Extraction and sequencing of RNA

P. aeruginosa strains were grown in LB-Mops broth at 37°C for 18 h (OD_{600} ≈ 3.8-4.0). Total RNA was isolated using TRIzol™ Reagent (Thermo Fisher Scientific). The quantity of extracted total RNA was measured using a NanoDropTM 1000 spectrophotometer (Thermo Fisher Scientific). Extracted RNA was treated with DNase (RQ1 RNase-free DNase I, Promega, Beijing, China) to remove traces of genomic DNA. The obtained total RNA (2 independent RNA samples per strain) was sent to Novagen (Tianjin, China) for stranded paired-end mRNA-seq sequencing using the Illumina Novaseq Platform.

Quantitative real-time PCR (qRT-PCR)

Total RNA of *P. aeruginosa* strains (LasR-null, LasR-RpoA* and LasR-MexT) was reverse transcribed using the HiScript II 1st Strand cDNA Synthesis Kit (Vazyme Biotech) following the manufacturer's instructions. The obtained cDNA was then used for qRT-PCR analysis. Reactions containing the SYBR qPCR Master Mix (Vazyme Biotech) were prepared in 96-well plates and run in a StepOnePlus Real-Time PCR System (Applied Biosystems, Waltham, MA, USA) as recommended by the supplier. Primers used for qRT-PCR are listed in Table S7. The measured values for a given gene were normalized to the expression level of the *proC* gene. Reactions were performed in triplicate.

Transcriptome analysis

P. aeruginosa strains (LasR-null, LasR-RpoA* and LasR-MexT, each strain has two replicates) were subjected to RNA-seq analysis. RNA-seq short reads were filtered with a customized Perl script to remove Illumina adapters and reads of low quality (Phred Score, $Q < 30$). The quality of filtered reads was assessed by FastQC. Trimmed reads were then mapped to the *P. aeruginosa* PAO1 reference genome (NC_002516.2) using Hisat2. The SAM files were further converted to BAM files by Samtools. Reads aligned to the reference genome were counted by HTSeq. The generated count files were further processed with the R package DESeq2. Genes were regarded as "differentially expressed" if they showed a fold change ≥ 2.0 and a P value ≤ 0.05.

Gene expression profile analysis

Genes showing 4-fold expression changes in strain comparisons were compared using customized R and Perl scripts. P values were computed using a one-sided KS test [50].

Used Software

The following software were used in this study:

BWA software, version 0.7.15-r1140 (http://bio-bwa.sourceforge.net) [51];

Cutadapt software, version 1.16 (https://github.com/mafdrcelm/cutadapt/) [52];

Samtools software, version 1.5 (http://samtools.sourceforge.net)[53];

FastQC, version fastqc_v0.11.5 (https://www.bioinformatics.babraham.ac.uk/projects/fastqc/);

Hisat2, version 2.1.0 (https://daehwankimlab.github.io/hisat2/) [54];

HTSeq, version 0.11.1 (https://htseq.readthedocs.io/en/release_0.11.1/count.html) [55];

DESeq2 [56];

Perl software, version v5.22.1 (https://www.perl.org/);

Python software, version v3.8.2 (https:// www. python. org/);

R software, version v3.6.1 (http://www.R-project.org/);

GraphPad Prism software, version 5 (https://www.graphpad.com/);

Image J software, version 1.8.0_172 (http://imagej.nih.gov/ij/).

Statistical analysis

Statistical analysis (*t*-test and KS tests) was performed using Excel and R software (http://www.R-project.org/).

Data Availability

RNA-seq data sets have been deposited in the NCBI SRA database (www.ncbi.nlm.nih.gov/sra) under the accession number PRJNA863086.

Authors' contributions

W.C., H.L., M.L., X.Z., X.C. and W.D. designed experiments. W.C., H.L., M.L., X.Z., X.C. and W.D. conducted the experiments. W.D. performed bioinformatics analyses. W.C., W.D. and C.S. wrote the manuscript. All authors reviewed the manuscript.

Competing interests

The authors declare that they have no competing interests.

Funding

This work was supported by the National Natural Science Foundation of China (31771341).

Acknowledgements

We are grateful to Eugene Makeyev (King's College London, UK) for providing useful assistances in bioinformatics analyses. We thank E. Peter Greenberg (University of Washington, USA) reading this manuscript and giving useful comments. We want to express our gratitude to all lab members for their assistances and supports with respect to many aspects of this work.

References

1. Gellatly, S.L. & Hancock, R.E. *Pseudomonas aeruginosa*: new insights into pathogenesis and host defenses. *Pathogens and disease* **67**, 159-173 (2013).
2. Klockgether, J. & Tümmler, B. Recent advances in understanding *Pseudomonas aeruginosa* as a pathogen. *F1000Research* **6** (2017).
3. Papenfort, K. & Bassler, B.L. Quorum sensing signal–response systems in Gram-negative bacteria. *Nat. Rev. Microbiol.* **14**, 576 (2016).
4. Lee, J. & Zhang, L. The hierarchy quorum sensing network in *Pseudomonas aeruginosa*. *Protein & cell* **6**, 26-41 (2015).
5. Schuster, M. & Greenberg, E.P. A network of networks: quorum-sensing gene regulation in *Pseudomonas aeruginosa*. *Int. J. Med. Microbiol.* **296**, 73-81 (2006).
6. Diggle, S.P., Cornelis, P., Williams, P. & Cámara, M. 4-quinolone signalling in *Pseudomonas aeruginosa*: old molecules, new perspectives. *Int. J. Med. Microbiol.* **296**, 83-91 (2006).
7. Pesci, E.C. et al. Quinolone signaling in the cell-to-cell communication system of *Pseudomonas aeruginosa*. *PNAS* **96**, 11229-11234 (1999).
8. Feltner, J.B. et al. LasR variant cystic fibrosis isolates reveal an adaptable quorum-sensing hierarchy in *Pseudomonas aeruginosa*. *MBio* **7**, e01513-01516 (2016).
9. Cruz, R.L. et al. RhlR-regulated acyl-homoserine lactone quorum sensing in a cystic fibrosis isolate of *Pseudomonas aeruginosa*. *MBio* **11** (2020).
10. Chen, R., Déziel, E., Groleau, M.-C., Schaefer, A.L. & Greenberg, E.P. Social cheating in a *Pseudomonas aeruginosa* quorum-sensing variant. *PNAS* **116**, 7021-7026 (2019).
11. Bjarnsholt, T. et al. Quorum sensing and virulence of *Pseudomonas aeruginosa* during lung infection of cystic fibrosis patients. *PloS one* **5**, e10115 (2010).

12. Sandoz, K.M., Mitzimberg, S.M. & Schuster, M. Social cheating in *Pseudomonas aeruginosa* quorum sensing. *PNAS* **104**, 15876-15881 (2007).
13. Diggle, S.P., Griffin, A.S., Campbell, G.S. & West, S.A. Cooperation and conflict in quorum-sensing bacterial populations. *Nature* **450**, 411-414 (2007).
14. Kostylev, M. et al. Evolution of the *Pseudomonas aeruginosa* quorum-sensing hierarchy. *PNAS* **116**, 7027-7032 (2019).
15. Oshri, R.D., Zrihen, K.S., Shner, I., Omer Bendori, S. & Eldar, A. Selection for increased quorum-sensing cooperation in *Pseudomonas aeruginosa* through the shut-down of a drug resistance pump. *ISME J* **12**, 2458-2469 (2018).
16. Smith, E.E. et al. Genetic adaptation by *Pseudomonas aeruginosa* to the airways of cystic fibrosis patients. *PNAS* **103**, 8487-8492 (2006).
17. Hoffman, L.R. et al. *Pseudomonas aeruginosa* lasR mutants are associated with cystic fibrosis lung disease progression. *Journal of Cystic Fibrosis* **8**, 66-70 (2009).
18. Ko□hler, T., Van Delden, C., Curty, L.K., Hamzehpour, M.M. & Pechere, J.-C. Overexpression of the MexEF-OprN multidrug efflux system affects cell-to-cell signaling in *Pseudomonas aeruginosa*. *J. Bacteriol.* **183**, 5213-5222 (2001).
19. Lister, P.D., Wolter, D.J. & Hanson, N.D. Antibacterial-resistant *Pseudomonas aeruginosa*: clinical impact and complex regulation of chromosomally encoded resistance mechanisms. *Clin. Microbiol. Rev.* **22**, 582-610 (2009).
20. Köhler, T., Epp, S.F., Curty, L.K. & Pechère, J.-C. Characterization of MexT, the regulator of the MexE-MexF-OprN multidrug efflux system of *Pseudomonas aeruginosa*. *J. Bacteriol.* **181**, 6300-6305 (1999).
21. Tian, Z.-X. et al. MexT modulates virulence determinants in *Pseudomonas aeruginosa* independent of the MexEF-OprN efflux pump. *Microb. Pathog.* **47**, 237-241 (2009).
22. Tian, Z.-X. et al. Transcriptome profiling defines a novel regulon modulated by the LysR-type transcriptional regulator MexT in *Pseudomonas aeruginosa*. *Nucleic Acids Res.* **37**, 7546-7559 (2009).
23. Richardot, C. et al. Amino acid substitutions account for most MexS alterations in clinical nfxC mutants of *Pseudomonas aeruginosa. Antimicrobial agents and chemotherapy* **60**, 2302-2310 (2016).
24. Sobel, M.L., Neshat, S. & Poole, K. Mutations in PA2491 (*mexS*) promote MexT-dependent mexEF-oprN expression and multidrug resistance in a clinical strain of *Pseudomonas aeruginosa*. *J. Bacteriol.* **187**, 1246-1253 (2005).
25. Ko¨ hler, T. et al. Characterization of MexE–MexF–OprN, a positively regulated multidrug efflux system of *Pseudomonas aeruginosa*. *Mol. Microbiol.* **23**, 345-354 (1997).
26. Gilbert, J. et al. Intestinal tissues induce an SNP mutation in *pseudomonas aeruginosa* that enhances its virulence: possible role in anastomotic leak. *PloS One* **7** (2012).
27. Cheng, X. et al. Spontaneous quorum-sensing hierarchy reprogramming in Pseudomonas aeruginosa laboratory strain PAO1. *AMB Express* **12**, 6 (2022).
28. Luong, P.M. et al. Emergence of the P2 phenotype in *Pseudomonas aeruginosa* PAO1 strains involves various mutations in *mexT* or *mexF*. *J. Bacteriol.* **196**, 504-513 (2014).
29. Köhler, T., Van Delden, C., Curty, L.K., Hamzehpour, M.M. & Pechere, J.-C. Overexpression of the MexEF-OprN multidrug efflux system affects cell-to-cell signaling in *Pseudomonas aeruginosa*. *J. Bacteriol.* **183**, 5213-5222 (2001).

30. Kulasekara, H.D. et al. A novel two-component system controls the expression of *Pseudomonas aeruginosa* fimbrial cup genes. *Mol. Microbiol.* **55**, 368-380 (2005).
31. Lee, S.A. et al. General and condition-specific essential functions of *Pseudomonas aeruginosa*. *PNAS* **112**, 5189-5194 (2015).
32. Lamarche, M.G. & Déziel, E. MexEF-OprN efflux pump exports the *Pseudomonas* quinolone signal (PQS) precursor HHQ (4-hydroxy-2-heptylquinoline). *PloS one* **6**, e24310 (2011).
33. Maseda, H., Yoneyama, H. & Nakae, T. Assignment of the substrate-selective subunits of the MexEF-OprN multidrug efflux pump of *Pseudomonas aeruginosa*. *Antimicrobial agents and chemotherapy* **44**, 658-664 (2000).
34. Köhler, T., Michea-Hamzehpour, M., Plesiat, P., Kahr, A.-L. & Pechere, J.-C. Differential selection of multidrug efflux systems by quinolones in *Pseudomonas aeruginosa*. *Antimicrobial agents and chemotherapy* **41**, 2540-2543 (1997).
35. Déziel, E. et al. Analysis of *Pseudomonas aeruginosa* 4-hydroxy-2-alkylquinolines (HAQs) reveals a role for 4-hydroxy-2-heptylquinoline in cell-to-cell communication. *PNAS* **101**, 1339-1344 (2004).
36. Rajaraman, E. et al. Transcriptional analysis and adaptive evolution of *Escherichia coli* strains growing on acetate. *Appl. Microbiol. Biotechnol.* **100**, 7777-7785 (2016).
37. Le Gac, M., Cooper, T.F., Cruveiller, S., Médigue, C. & Schneider, D. Evolutionary history and genetic parallelism affect correlated responses to evolution. *Mol. Ecol.* **22**, 3292-3303 (2013).
38. Murayama, S., Ishikawa, S., Chumsakul, O., Ogasawara, N. & Oshima, T. The role of α-CTD in the genome-wide transcriptional regulation of the *Bacillus subtilis* cells. *PloS one* **10**, e0131588 (2015).
39. Murakami, K., Fujita, N. & Ishihama, A. Transcription factor recognition surface on the RNA polymerase alpha subunit is involved in contact with the DNA enhancer element. *The EMBO Journal* **15**, 4358-4367 (1996).
40. Gaal, T. et al. DNA-binding determinants of the alpha subunit of RNA polymerase: novel DNA-binding domain architecture. *Genes Dev.* **10**, 16-26 (1996).
41. Finney, A.H., Blick, R.J., Murakami, K., Ishihama, A. & Stevens, A.M. Role of the C-terminal domain of the alpha subunit of RNA polymerase in LuxR-dependent transcriptional activation of the lux operon during quorum sensing. *J. Bacteriol.* **184**, 4520-4528 (2002).
42. Schweizer, H.P. Efflux as a mechanism of resistance to antimicrobials in *Pseudomonas aeruginosa* and related bacteria: unanswered questions. *Genet Mol Res* **2**, 48-62 (2003).
43. Winstanley, C., O'Brien, S. & Brockhurst, M.A. *Pseudomonas aeruginosa* evolutionary adaptation and diversification in cystic fibrosis chronic lung infections. *Trends Microbiol.* **24**, 327-337 (2016).
44. Huang, H. et al. An integrated genomic regulatory network of virulence-related transcriptional factors in *Pseudomonas aeruginosa*. *Nature communications* **10**, 1-13 (2019).
45. Kim, M.-K. & Harwood, C.S. Regulation of benzoate-CoA ligase in *Rhodopseudomonas palustris*. *FEMS Microbiol. Lett.* **83**, 199-203 (1991).
46. Rietsch, A., Vallet-Gely, I., Dove, S.L. & Mekalanos, J.J. ExsE, a secreted regulator of type III secretion genes in *Pseudomonas aeruginosa*. *PNAS* **102**, 8006-8011 (2005).

47. Stover, C.K. et al. Complete genome sequence of *Pseudomonas aeruginosa* PAO1, an opportunistic pathogen. *Nature* **406**, 959-964 (2000).
48. Choi, K.-H. & Schweizer, H.P. mini-Tn 7 insertion in bacteria with single att Tn 7 sites: example *Pseudomonas aeruginosa*. *Nature protocols* **1**, 153 (2006).
49. Lenski, R.E., Rose, M.R., Simpson, S.C. & Tadler, S.C. Long-term experimental evolution in *Escherichia coli*. I. Adaptation and divergence during 2,000 generations. *The American Naturalist* **138**, 1315-1341 (1991).
50. Lim, L.P. et al. Microarray analysis shows that some microRNAs downregulate large numbers of target mRNAs. *Nature* **433**, 769-773 (2005).
51. Li, H. & Durbin, R. Fast and accurate short read alignment with Burrows–Wheeler transform. *Bioinformatics* **25**, 1754-1760 (2009).
52. Martin, M. Cutadapt removes adapter sequences from high-throughput sequencing reads. *EMBnet. journal* **17**, 10-12 (2011).
53. Li, H. et al. The sequence alignment/map format and SAMtools. *Bioinformatics* **25**, 2078-2079 (2009).
54. Kim, D., Langmead, B. & Salzberg, S.L. HISAT: a fast spliced aligner with low memory requirements. *Nat. Methods* **12**, 357-360 (2015).
55. Anders, S., Pyl, P.T. & Huber, W. HTSeq—a Python framework to work with high-throughput sequencing data. *Bioinformatics* **31**, 166-169 (2015).
56. Love, M.I., Huber, W. & Anders, S. Moderated estimation of fold change and dispersion for RNA-seq data with DESeq2. *Genome Biology* **15**, 550 (2014).

Figure legends

Figure 1. Scheme illustrating the novel TGD-MS strategy.

(A) Illustration of the overall procedure of TGD-MS strategy developed in our study aims to discover mutations in none-*mexT* genes. The evolution experiment is initiated with a QS-inactive recombinant LasR-null mutant an extra copy of *mexT*. The bacteria are spread on skim milk agar plates to select for QS-active revertants secreting QS-dependent proteases. This screening method results in identification of mutations in genes other than *mexT*. (B). The predicted genotype changes in colonies in the course of evolution with TGD-MS strategy. The probability of obtaining *mexT* mutants from skim milk agar plates is reduced by introducing an extra copy of *mexT* into the LasR-null mutant, thus facilitating the selection of colonies containing mutations in QS-reprogramming regulator genes other than *mexT*. QS-, inactive QS; QS+, active QS.

Figure 2. Identification of QA-active mutants obtained from a LasR mutant with an extra copy of *mexT*.

(A) Frequency of protease-positive colonies obtained from three TGD-MS experiments with the LasR mutant carrying an extra copy of *mexT*. Bacterial colonies were selected and examined for extracellular protease activity at different time points using skim milk agar plates. (B) Pyocyanin production in identified protease-positive colonies. Pyocyanin production (OD_{695}/OD_{600} values) was quantified for each strain (LasR-null, LasR-null mutant used as a negative control; LasR-1/2/3/4, obtained mutants displaying protease-positive phenotype and significantly increased pyocyanin production). Data are presented as means ± SD ($n = 3$). ***$P < 0.001$ (t-test).

Figure 3. The LasR-RpoA* mutant shows increased QS-related activities

(A-B) Rhl- (A) and PQS-responsive (B) QS activities of indicated strains. Rhl- and PQS-responsive QS activities are reflected by the fluorescence levels of the expressed reporters P*rhlA*-GFP and P*pqsA*-GFP, respectively. Fluorescence values, expressed as relative fluorescence units (RFU), were obtained from bacteria cultured for 18 h. (C-D) Relative concentration of C4-HSL(C) and PQS (D) in the shown strains. Production of AHLs in wild-type (WT) PAO1 was set to 100%. (E) Pyocyanin production (OD_{695}/OD_{600} values) in these strains. (F) Cyanide production by these strains. Image J software was used to compare the amount of produced cyanide. The cyanide-sensitive filter papers were photographed after growth of the bacteria in 6-well plates at 37 °C for 18 h. The amount of cyanide produced in wild-type PAO1 was set to 100%. Data are presented as means ± SD (n = 3, t-test). *P < 0.05, **P < 0.01, ***P < 0.001 (t-test).

Figure 4. Transcriptome analysis of the LasR-RpoA* mutant

(A) Volcano plots showing the magnitude of differential gene expression induced by the identified T262→A mutation in *rpoA* (transcriptome comparison of LasR-RpoA* compared to the parent strain LasR-null). Each dot represents one annotated sequence with detectable expression (red dots, up-regulated genes; blue dots, down-regulated genes; green dots, genes that are not differentially expressed). Thresholds for defining a gene significantly differentially expressed (log2 (fold change) ≧ |1.0|, P value ≦0.05) are shown as dashed lines. (B-C) Expression levels of genes in QS-related genes (B) and of efflux pump genes of the *mexEF-oprN* operon (C). A positive log2 (fold change) value indicates up-regulation and a negative value indicates down-regulation of a given gene in the LasR-RpoA* mutant compared to LasR-null. Data are indicate means ± SD.

Figure 5. RpoA* modulates expression of *mexEF-oprN* operon genes.

(A) The LasR-RpoA* mutant shows reduced transcription of *mexEF-oprN* operon genes as estimated with the help of P*mexE*-GFP, a *mexEF* promoter-GFP fusion construct. Data of indicated strains are presented as means ± SD. *P < 0.05, **P < 0.01, ***P < 0.001 (t-test). (B) Illustration of the probe DNA used for the performed EMSA with recombinant RpoA of wild-type (WT) bacteria or RpoA*. (C) EMSA results showing that RNAP containing RpoA forms a DNA-protein complex. A weaker signal is seen for the sample with recombinant RpoA*. The unbound probe DNA is seen at the bottom of the blot.

Figure 6. Effects of chloramphenicol on the growth fitness of the LasR-RpoA* mutant.

The LasR-RopA* and LasR-MexT mutants were labeled with a Gm resistance gene (pUC18T-mini-Tn7T-Gm). Each mutant was then co-cultured with the LasR-null mutant at a start ratio of 5:95 in PM-casein medium containing indicated concentrations of chloramphenicol. After incubation for 48 h, colonies were counted and relative fitness (w) was estimated by determining the ratio of Malthusian growth parameters.

Figure 7. Transcriptional regulation of *mexEF-oprN* operon genes.
Transcription of *mexEF-oprN* operon genes is positively regulated by the transcriptional regulator MexT and requires RNAP consisting of a small α-subunit (RpoA containing a C-terminal and an N-terminal domain; α-CTD, α-NTD), large β- and β′-subunits, a small ω subunit and a promoter recognizing σ-subunit (sigma factor). MexT is negatively regulated by MexS. The QS-active LasR-RpoA* and LasR-MexT mutants show reduced transcription of *mexEF-oprN* operon genes. LasR-null mutants with mutated *mexE* or with a transposon insertion in *mexF* also exhibit a QS-active phenotype.

Figure 8. Iterative application of the TGD-MS method.
Schematic representation of the iterative application of the TGD-MS approach**.** (A) Under evolutionary pressure, mutations in genes of metabolic pathways can lead to phenotype changes over time. Genetic components and redundancy of similar pathways may contribute to phenotypic robustness. (B) Iterative use of the TGD-MS method. Additional copies of already identified genes of a given pathway are introduced into the strain to "block" the occurrence of colonies mutated in these genes in the evolution experiment. This accelerates identification of novel genes of a given pathway. TGD-MS iterations may also result in identification of alternative pathways as the screening stringency steadily increases with each round of the evolution experiment.

Supplementary Figures

Figure S1. The constructed LasR-RpoA* mutant exhibits elevated proteolytic activity.
(A) Equal numbers of bacteria of indicated strains were spotted on skim milk plates to estimate proteolytic activity resulting in transparent proteolytic zones (halos). Pictures were taken 24 h later. (B) Quantification of proteolytic zones shown (A). Data represent means ± SD (n = 3). *P < 0.05, **P < 0.01, ***P < 0.001 (t-test).

Figure S2. The RpoA* mutation significantly enhances host cell cytotoxicity.
The killing assay with human lung carcinoma A549 cells was performed with equal amounts of indicated strains. After incubation for 6 h, the release of cytosolic lactate dehydrogenase (LDH) from the A549 cells was quantified. The released amount of LDH inoculated with wild-type PAO1 (WT) was set to 100%. Data represent means ± SD (n = 3). *P < 0.05, **P < 0.01, ***P < 0.001 (t-test).

Figure S3. Complementation of the LasR-RpoA* mutant with a wild-type *rpoA* gene reduces QS-related activities.
Introduction of an episomal copy of the wild-type *rpoA* gene into the LasR-RpoA* mutant diminished the QS-controlled proteolytic activity and pyocyanin production. (A) Proteolytic activity as visualized by the skim milk plate assay. Photographs of indicated strains were taken after transfer of equal amounts of bacteria onto the skim milk plate and incubation at 37 ^{o}C for 24 h. (B) Pyocyanin production of indicated strains. The LasR-null mutant or the LasR-RpoA* mutant was either transformed with the empty vector pJN105 (Ctr) or the RpoA-expressing vector pJN105-RpoA (RpoA).

Expression of *rpoA* was induced by addition of 1 mg/ml L-arabinose. Data represent means ± SD (n = 3). *P < 0.05, **P < 0.01, ***P < 0.001 (t-test).

Figure S4. qRT-PCR validation of differentially expressed genes obtained from the transcriptomic analysis.

The qRT-PCR validation of differentially expressed genes obtained from the transcriptome analysis. Relative expression was normalized using *proC* gene data. Data represent means ± SD (3 independent RNA extractions; n = 3). *P < 0.05, **P < 0.01, ***P < 0.001 (t-test).

Figure S5. Swarming motility in the LasR-RpoA* mutant.

(A) Bacterial swarming motility was assayed on 0.5% agar plates. Plates were photographed after incubation at 37 ^{o}C for 18 h. Representative photographs are shown for indicated mutant strains (LasR-null-Ctr, the LasR-null mutant carrying the empty pJN105 vector; LasR-RpoA*-Ctr, the LasR-RpoA* mutant carrying the empty pJN105 vector; LasR-RpoA*-RpoA, the LasR-RpoA* mutant complemented with pJN105-RpoA containing wild-type *rpoA*). (B) Quantification of diameters in formed colonies. The *rpoA* gene expression was induced by addition of L-arabinose (1 mg/ml). Data indicate means ± SD from a representative experiment (n = 3). P values were obtained from t-tests. *P < 0.05, **P < 0.01, ***P < 0.001.

Figure S6. Deletion of *pqsA* in LasR-RpoA* reduces RpoA*-mediated extracellular protease activity.

(A) Extracellular proteolytic activity was visualized through spotting equal amounts of indicated strains on skim milk agar plates. Plates were photographed after incubation at 37 ^{o}C for 24 h and representative photos are shown. (B) Quantification of proteolytic zones obtained from obtained pictures. Data represent means ± SD (n = 3). *P < 0.05, **P < 0.01, ***P < 0.001 (t-test).

Supplementary Tables

Table S1. *lasR* and *mexT* mutations in isolates from chronically infected CF patients.

Table S2. Read mapping statistics of whole-genome re-sequencing data.

Table S3. Identification of mutations in protease-positive colonies derived from the LasR-null mutant with an extra copy of *mexT*.

Table S4. Genes differentially expressed in the LasR-RpoA* mutant compared to the LasR-null parent strain.

Table S5. Genes differentially expressed in the LasR-MexT mutant compared to the LasR-null parent strain.

Table S6. Strains and plasmids used in this study.

Table S7. Oligonucleotides used in this study.

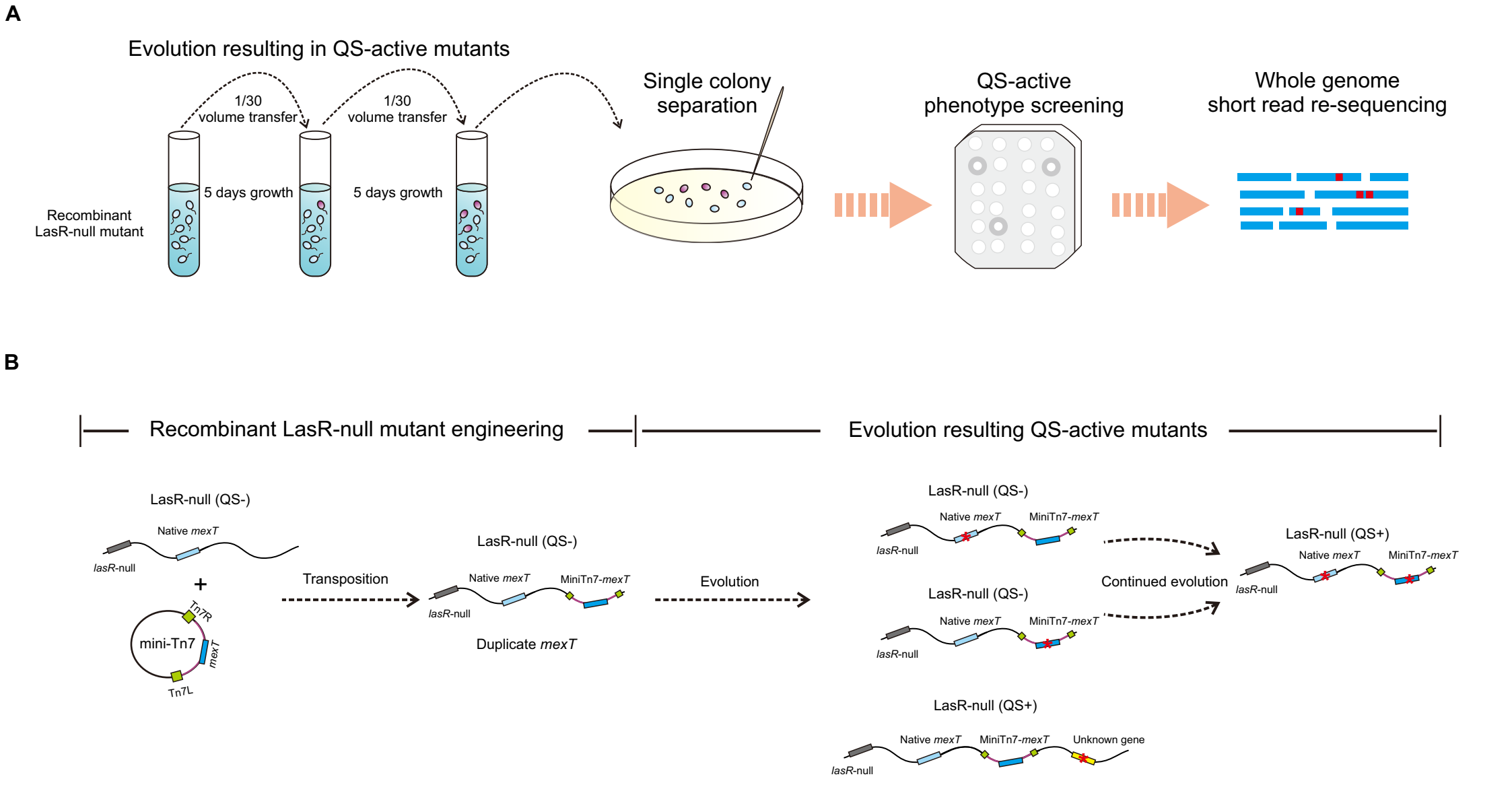
A
Evolution resulting in QS-active mutants
1/30
volume transfer
1/30
volume transfer
Recombinant
LasR-null mutant
5 days growth
5 days growth
Single colony
separation
QS-active
phenotype screening
Whole genome
short read re-sequencing
B
Recombinant LasR-null mutant engineering
Evolution resulting QS-active mutants
LasR-null (QS-)
Native mexT
lasR-null
+
mini-Tn7
Tn7R
mexT
Tn7L
Transposition
LasR-null (QS-)
Native mexT
MiniTn7-mexT
lasR-null
Duplicate mexT
Evolution
LasR-null (QS-)
Native mexT
MiniTn7-mexT
lasR-null
LasR-null (QS-)
Native mexT
MiniTn7-mexT
lasR-null
Continued evolution
LasR-null (QS+)
Native mexT
MiniTn7-mexT
lasR-null
LasR-null (QS+)
Native mexT
MiniTn7-mexT
Unknown gene
lasR-null

Fig. 1

A

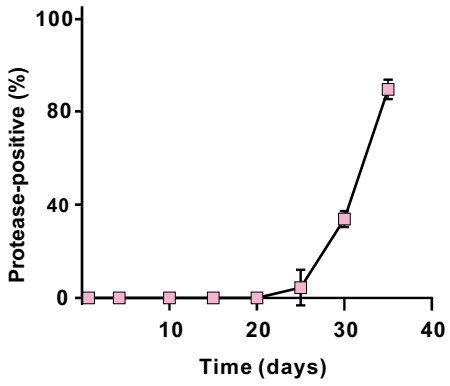
Protease-positive (%)
100
80
40
0
10
20
30
40
Time (days)

B

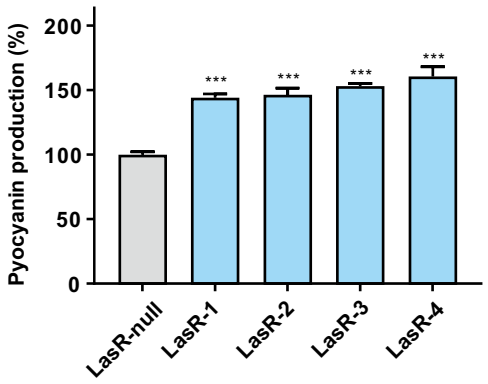
Pyocyanin production (%)
200
150
100
50
0
***
***
***
***
LasR-null
LasR-1
LasR-2
LasR-3
LasR-4

Fig.2

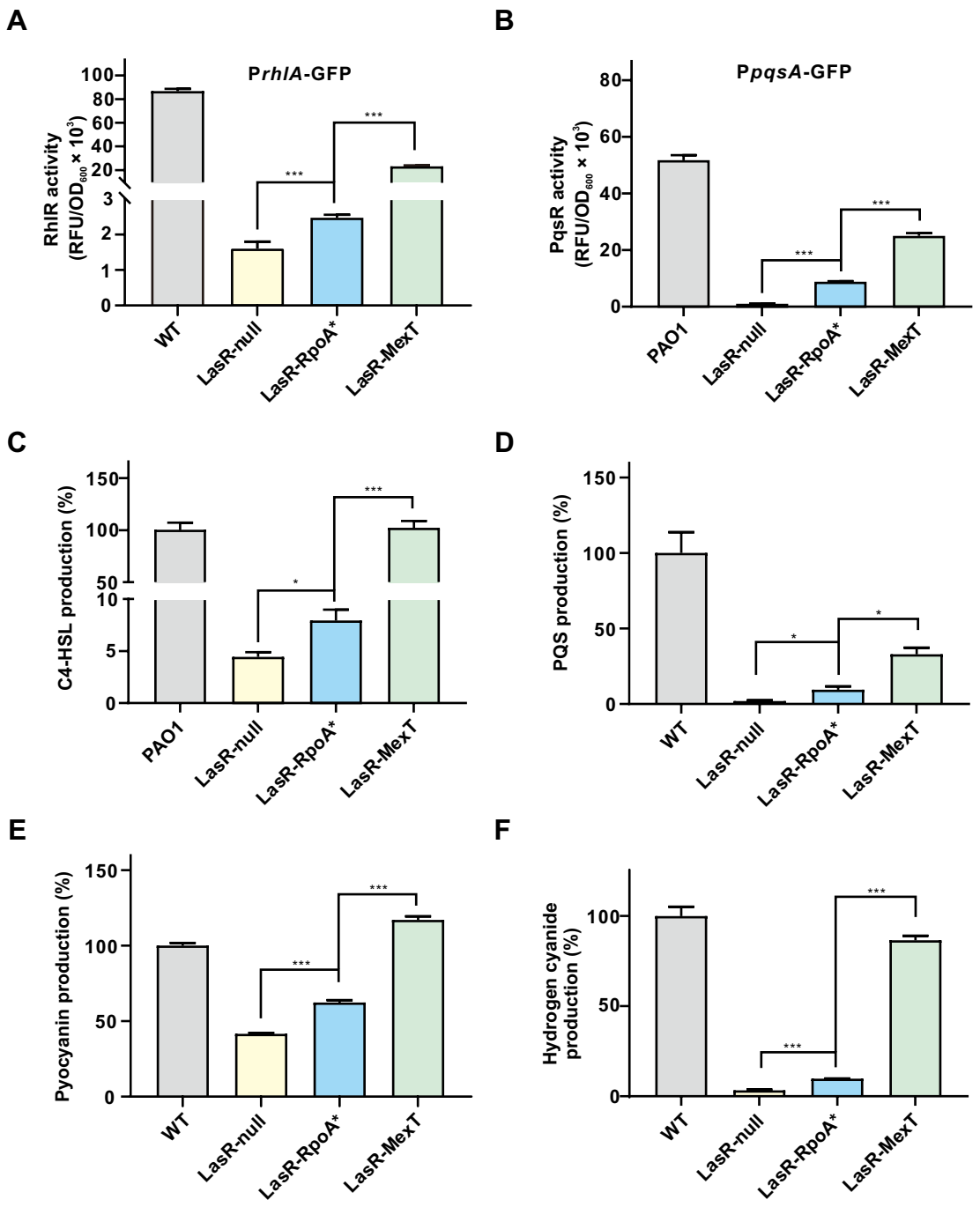
A
PrhlA-GFP
RhlR activity (RFU/OD600 × 10^3)
100
80
60
40
20
3
2
1
0
***
***
WT
LasR-null
LasR-RpoA*
LasR-MexT
B
PpqsA-GFP
PqsR activity (RFU/OD600 × 10^3)
80
60
40
20
0
***
***
PAO1
LasR-null
LasR-RpoA*
LasR-MexT
C
C4-HSL production (%)
150
100
50
10
5
0
***
*
PAO1
LasR-null
LasR-RpoA*
LasR-MexT
D
PQS production (%)
150
100
50
0
*
*
WT
LasR-null
LasR-RpoA*
LasR-MexT
E
Pyocyanin production (%)
150
100
50
0
***
***
WT
LasR-null
LasR-RpoA*
LasR-MexT
F
Hydrogen cyanide production (%)
100
50
0
***
***
WT
LasR-null
LasR-RpoA*
LasR-MexT

Fig.3

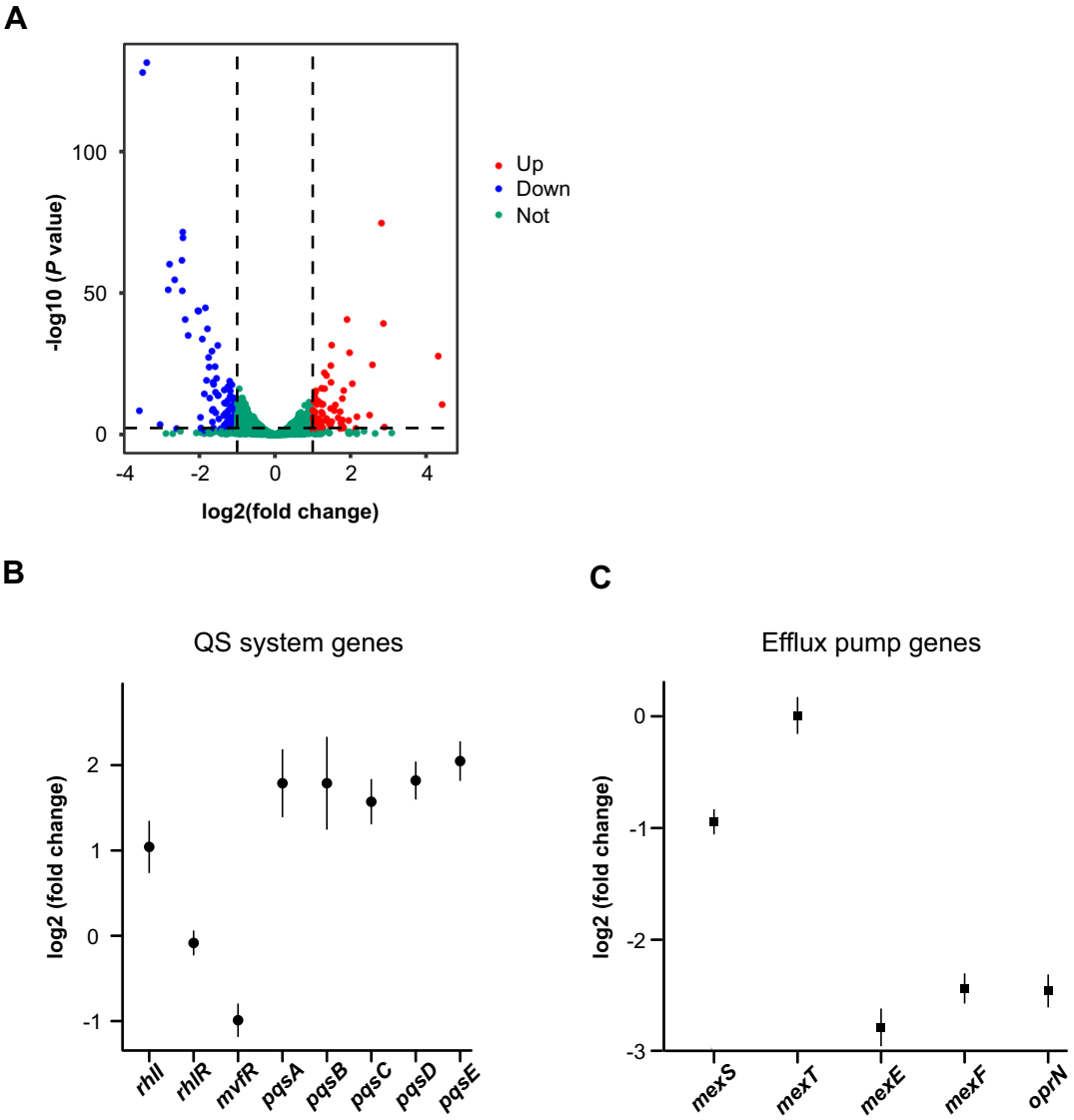
A
-log10 (P value)
100
50
0
-4
-2
0
2
4
log2(fold change)
Up
Down
Not
B
QS system genes
log2 (fold change)
2
1
0
-1
rhlI
rhlR
mvfR
pqsA
pqsB
pqsC
pqsD
pqsE
C
Efflux pump genes
log2 (fold change)
0
-1
-2
-3
mexS
mexT
mexE
mexF
oprN

Fig. 4

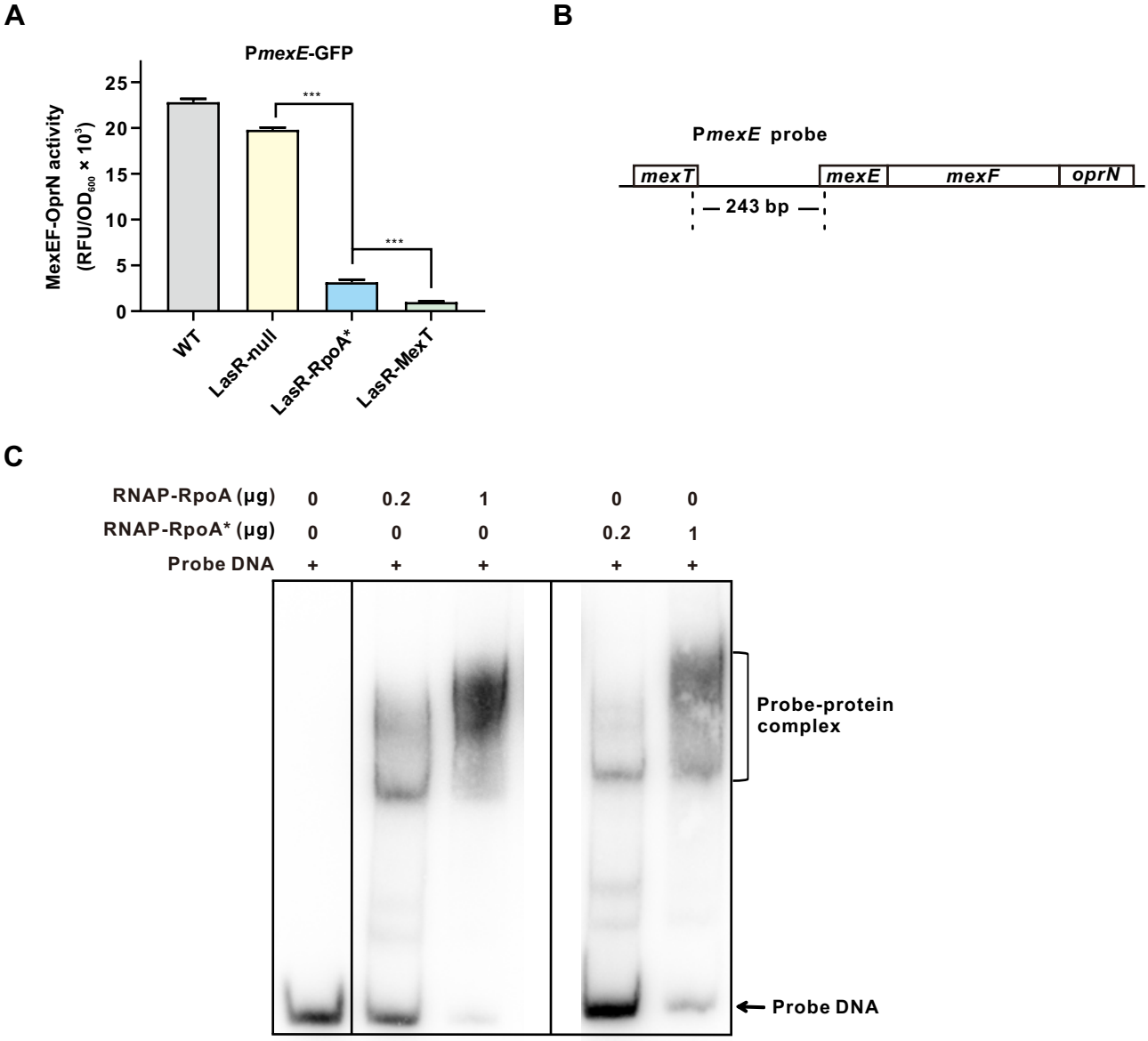
A
PmexE-GFP
MexEF-OprN activity
(RFU/OD600 × 10^3)
25
20
15
10
5
0
***
***
WT
LasR-null
LasR-RpoA*
LasR-MexT
B
PmexE probe
mexT
mexE
mexF
oprN
243 bp
C
RNAP-RpoA (μg) 0 0.2 1 0 0
RNAP-RpoA* (μg) 0 0 0 0.2 1
Probe DNA + + + + +
Probe-protein complex
Probe DNA

Fig. 5

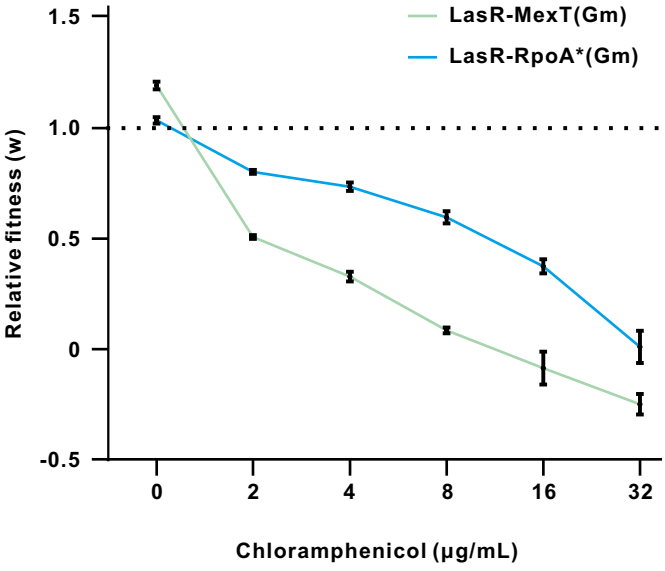
LasR-MexT(Gm)
LasR-RpoA*(Gm)
Relative fitness (w)
1.5
1.0
0.5
0
-0.5
0
2
4
8
16
32
Chloramphenicol (µg/mL)

Fig. 6

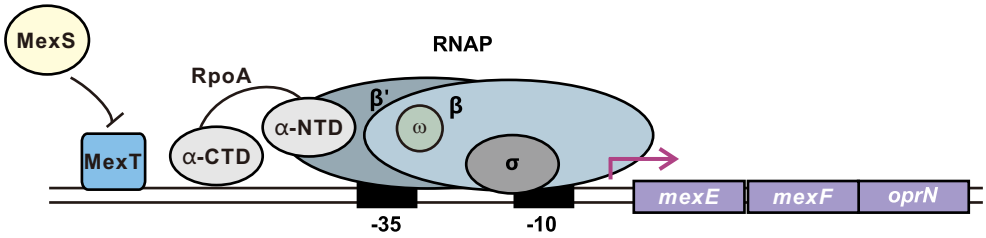

Fig.7

ω

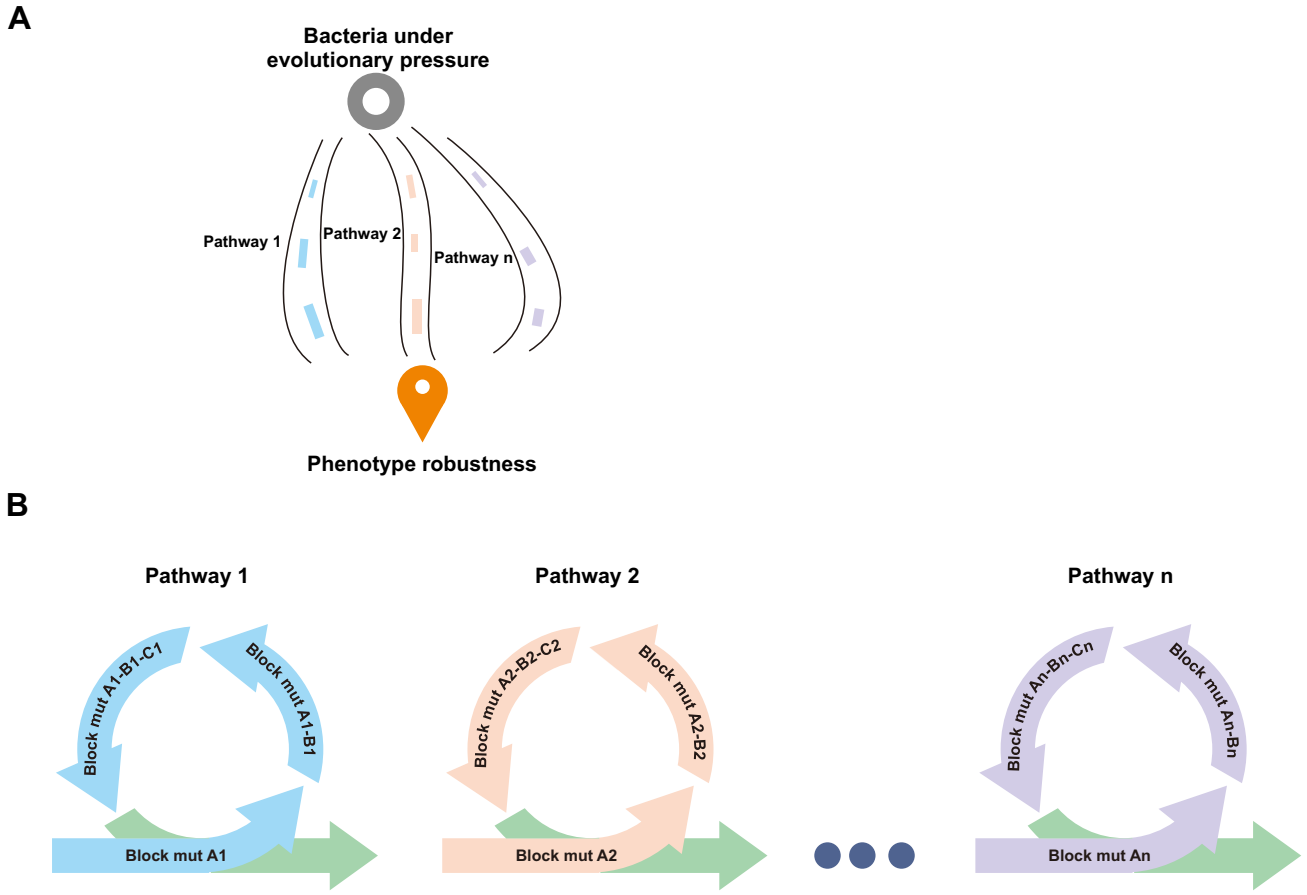
A
Bacteria under evolutionary pressure
Pathway 1
Pathway 2
Pathway n
Phenotype robustness
B
Pathway 1
Pathway 2
Pathway n
Block mut A1-B1-C1
Block mut A1-B1
Block mut A1
Block mut A2-B2-C2
Block mut A2-B2
Block mut A2
Block mut An-Bn-Cn
Block mut An-Bn
Block mut An

Fig. 8

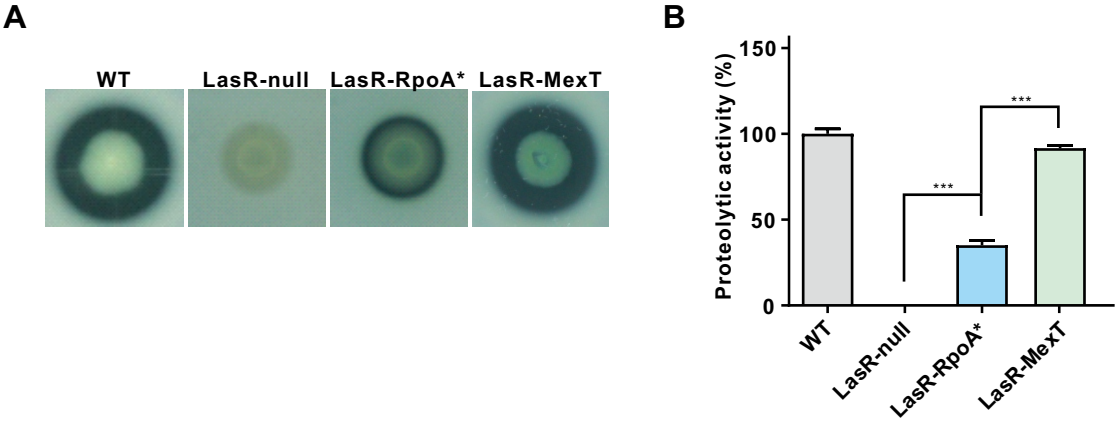
A
WT
LasR-null
LasR-RpoA*
LasR-MexT
B
Proteolytic activity (%)
150
100
50
0
***
***
WT
LasR-null
LasR-RpoA*
LasR-MexT

Fig.S1

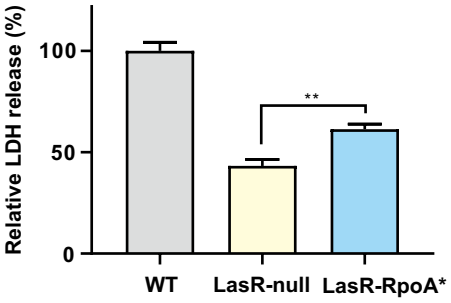

Fig. S2

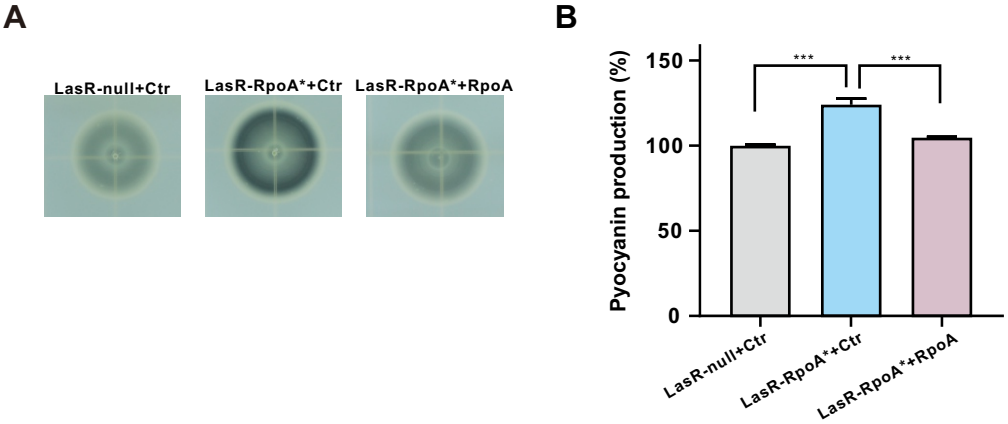
A
LasR-null+Ctr
LasR-RpoA*+Ctr
LasR-RpoA*+RpoA
B
Pyocyanin production (%)
150
100
50
0
***
***
LasR-null+Ctr
LasR-RpoA*+Ctr
LasR-RpoA*+RpoA

Fig.S3

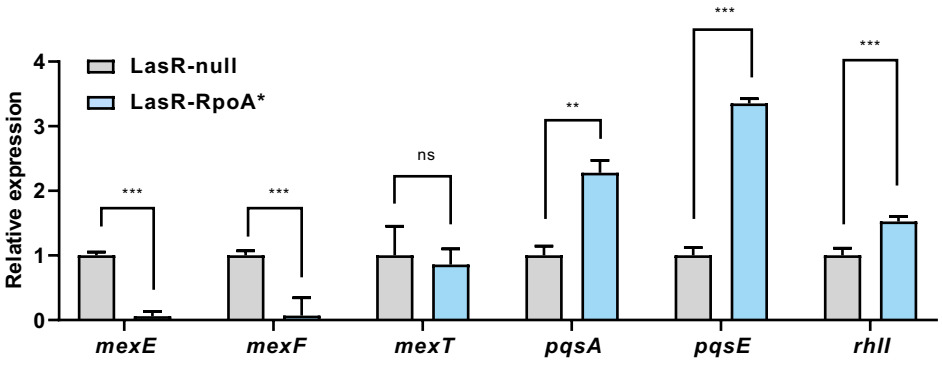
LasR-null
LasR-RpoA*
Relative expression
0
1
2
3
4
***
***
ns
**
***
***
mexE
mexF
mexT
pqsA
pqsE
rhlI

Fig. S4

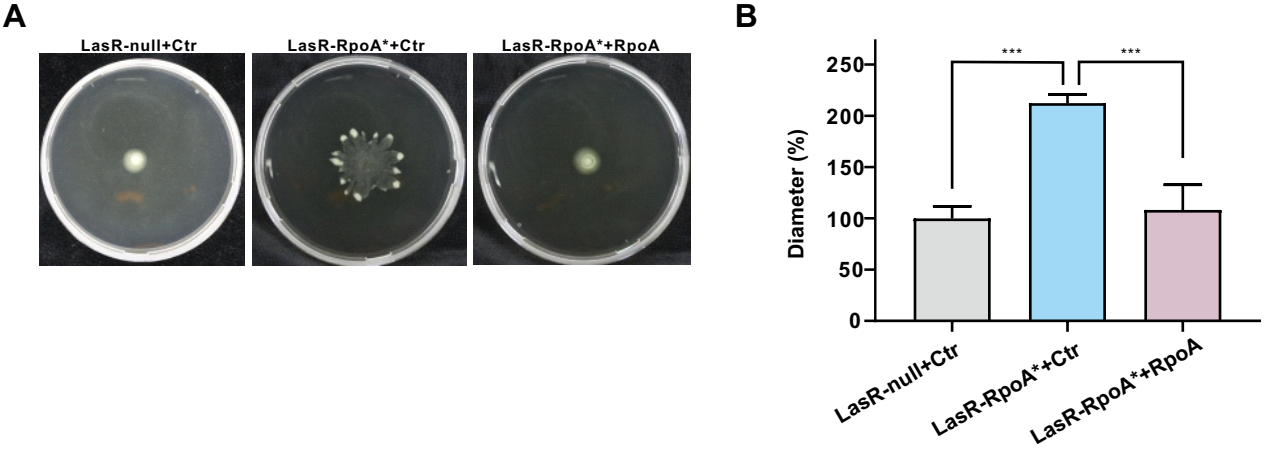
A
LasR-null+Ctr
LasR-RpoA*+Ctr
LasR-RpoA*+RpoA
B
Diameter (%)
250
200
150
100
50
0
***
***
LasR-null+Ctr
LasR-RpoA*+Ctr
LasR-RpoA*+RpoA

Fig. S5

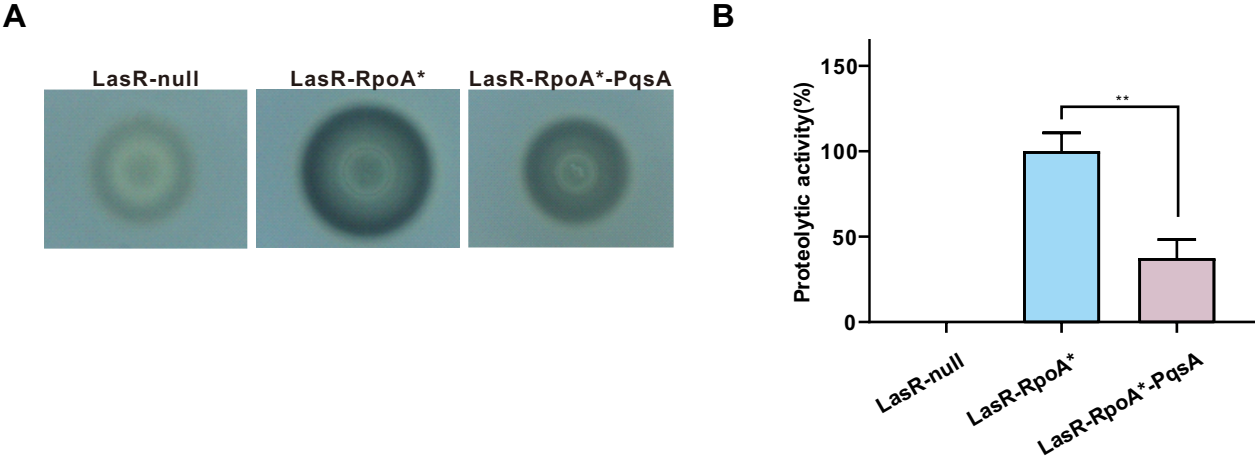
A
LasR-null
LasR-RpoA*
LasR-RpoA*-PqsA
B
Proteolytic activity(%)
150
100
50
0
**
LasR-null
LasR-RpoA*
LasR-RpoA*-PqsA

Fig. S6